Advances in Engineering Research, volume 209
International Joint Conference on Science and Engineering 2021 (IJCSE 2021)

Influence of Distance Between Nails on Strong Bending of Laminated Wood Beams-Meranti Wood and Sengon Wood

Suprapto Suprapto[1,*] Suparji Suparji[1] Ekohariadi Ekohariadi[2] Reza B. Aditya[1] Setya C.Wibawa[2]

[1]*Building Engineering Education, Faculty of Engineering, Universitas Negeri Surabaya, Indonesia*
[2]*Informatics Department, Universitas Negeri Surabaya, Indonesia*
[*]*Corresponding email: suprapto@unesa.ac.id*

ABSTRACT
Using nails as adhesive materials on meranti wood laminate beams and zinc wood is an attempt to anticipate the problems arising in laminate beams if using glue adhesives, which the laminate process can occur ideally. Improved mechanical possessions such as strong bending and elastic modulus can be achieved. They can be considered to recommend using meranti wood laminate beams and zinc on wood as other raw materials reviewed from technological and economic features. The purpose of this education was to find out the effect of the distance of the nail on the solid bending of laminated wood beams-mechanical meranti wood and sengon wood. The bending testing method used is one point landing with variations in nail adhesive distances of 10 cm, 15 cm, 20 cm, 25 cm, and 30 cm. The dimensions of the test object are 4 cm x 6 cm in thickness. Each lamina is 2 cm with a beam length of 150 cm. The lamina preparation is used in the press and pull area using meranti wood while in the middle using zinc on wood. In addition to load data that test objects can receive, the amount of exposure that occurs is also measured using a dial gauge placed under the test object at 1/3 the length of the right and left span and in the middle of the span. The results showed that the distance of the nail affects the strong bending of the laminate beam. The laminated beam nail space effect shows that the longer the nail is used, the less pliable. The damage that occurs also indicates that the longer the length of the nail used, the more damage that occurs leads to shear. The best nail spacing result used is a nail distance of 10cm with a bending power of 618.75 kg / cm², at that distance, the size of the bending is quite large close to the strength of the base material of the outermost layer of laminate-mechanical beams while wood is 98%. So it can be concluded that distance nails as an adhesive on laminate-mechanical wood beams influence the strong bending. The greater the distance of the nail used, the more minor the bending.

Keywords: *Distance of nail, Strong bending, Laminate-mechanical beam, Adhesive, Flexible strength*

1. INTRODUCTION

Wood is the most widely used physical for construction purposes. Wood is still much in demand in construction work because it has several advantages; among others, it has a specific strength that is high, light, easy to obtain. The price is relatively low in certain areas, and its implementation is straightforward. The age of cutting down old wood trees and forest land decreases, so the supply of wood for good quality large dimensional structures is reduced. Its high electrical conductivity, large surface area, excellent electrochemical properties, and calm strength [1]. Fiber-based biomass has become one of the most used filler materials for composite groundwork. It is a relatively cheap material, is often discarded as waste, and has residues from forestry and agricultural industries. The cellulose fiber structure offers low density and high specific strength and stiffness and is non-toxic to humans and nature [2]. The attachment strength is quantified, and the compatibility of the concept for the fabrication of a new generation of inertial microfluidic devices is evaluated using cells and atoms [3]. These defects may be detrimental to corrosion resistance, strength, and machinability [4].

The laminate process's success is influenced by several aspects, including glued materials, adhesive materials, and gluing technology. Different carbon fiber fabrics were used to analyze the plies and

laminates' mechanical parameters [5]. The compatibility between adhesives, material properties, and gluing techniques is a foundation for the success and quality of laminated crops. The strength of attachment can be used as a benchmark for the success of laminate production. Laminates generally use glue adhesives as a link between each lamina. Still, the problem that often arises is that glue adhesives sometimes cannot be perfectly attached to each lamina so that the laminate process does not occur. Demonstrations of the flexural strength of these armor-plated concrete beams are cast with different combinations [6]. Payable to these attractive possessions, Airy beams have many potential photonics applications, such as particle manipulation [7].

In addition to using adhesive, laminate beams can also use nails or bolts or a combination of adhesive with bolts or nails as a link between the lamination. This type of beam is known as an automatic laminate beam. These advances suggest that using platelet particles as adhesives provides a promising way to construct complex tissue engineering models using calcium-alginate hydrogels to regenerate different tissues [8]. Electroactivity and biocompatibility are appropriate. They have broad applications in tissue regeneration, electrostimulation, and bioelectronics implants [9]. Rapid advances allow new fabrication methods of adhesive electronic patches to be stretched [10]. Through the results of experimental characterizations and theoretical simulations, this bionic interface layer accurately controls the crystallization and acts as an adhesive [11]. After it adheres to wet tissues, the bioadhesive becomes a tough hydrogel with mechanical compliance and stretchability comparable with those of soft tissues [12]

The study of nails as adhesive materials on meranti wood laminate beams and zinc wood is an attempt to anticipate the problems arising in laminate beams if using glue adhesives so that the laminate process can occur ideally. Better mechanical properties such as string bending and elastic modulus can be achieved. They can be considered to recommend using meranti wood laminate beams and zinc on wood as alternative raw materials reviewed from technological and economic aspects. The cleaning process removes microorganisms mechanically and chemically, thereby reducing the microbial load in this environment [13]. It prevented mechanical memorization of the correct variant and led to the analysis of mistakes [14]. However, due to the limited period of the class, the mechanical breakdown of the connection joint is not described [15].

Laminated beams are structural products used for CWC frames, beams, columns, and horses. This technique is suitable for nonlaminated and uncoated wood-based panels [16]. However, this matter is inverse in its higher value. Ply point of view, nonlocality, and distance scale on micro-wobble of laminated compounds visible [17]. We extend the ultrastrong graphene papers to the realistic laminated composites and achieve high strength combined with attractive conductive and electromagnetic shielding performance [18].

According to PKKI NI-5 1961 in the list of Indonesian wood, meranti wood has many types and variations and belongs to the strong class ii-IV type with an average type weight of 0.55 gr / cm^3. As zinc on wood has a lot of kinds and varieties and belongs to the kind of solid class IV-V with an average type weight of 0.33 gr / cm^3. Therefore, research must be done researching the characteristics of meranti wood and sengon wood used to know the characteristics of wood both from physical and mechanical properties. Their unique properties determine the use of nanocomposites due to the vast specific surface and high surface energy of nanoparticles. Nanometer particles, unlike micro-and more extensive inclusions, do not stress concentrators, which contributes to a significant increase in the mechanical properties of nanocomposites [19]. Individuals were classified as having or not having mechanical complications, and reduction quality and radiologic outcomes were compared between the two groups [20]. This membrane's excellent mechanical strength and well-distributed nickel atoms combine gas-diffusion and catalyst layers into one architecture [21] due to its excellent mechanical and electrical properties [22].

The primary test of laminate-mechanical beams is by bending testing so that the bending strength on the shaft can be calculated using the following equations :

$$\sigma_{lt\perp} = \frac{M}{W} = \frac{M \times y}{I} \quad \text{.....1)}$$

For the appearance of a square, the size of the (side h > b, vertical), then:

$$I = I_x = \frac{1}{12} bh^3 \quad \text{.....2)}$$

$$y_a = y_b = \frac{1}{2} h = y \quad \text{..... 3)}$$

$$W_a = W_b = \frac{1}{6} bh^2 = W \quad \text{..... 4)}$$

If the beam with the focus of the roller-joint receives a centralized load in the middle of the span, then the equation of bending and deflection voltage is (SNI 03-3959-1995):

$$\Sigma_{lt\perp} = \frac{3PL}{2bh^2} \quad \text{..... 5)}$$

Where:
$\sigma_{lt\perp}$ = Flexure (kg/cm²)
M= Maximum moment
W = Retaining moment ($cm^{3)}$
y = Distance of the neutral line of the x axis to the end of the beam (cm)
I = Moment of inertia ($cm^{4)}$
P = Maximum load (kg)
L = Length of beam span (cm)
b = Beam width (cm)
h = Beam height (cm)

A connection with a nail has several advantages over a relationship with a bolt. Is related, among others, to the greater efficiency of nails, the weakening given is relatively small, which is about 10%, so it is often ignored, stiffer. The artistry is somewhat easier if the wood to be done is not too hard and the corresponding parts are not too thick, so it does not need to be drilled first. Nails are installed on at least two rows of pins. The density of tacks, overlap length, and butt joint affect the bending strength and rigidity of the element.

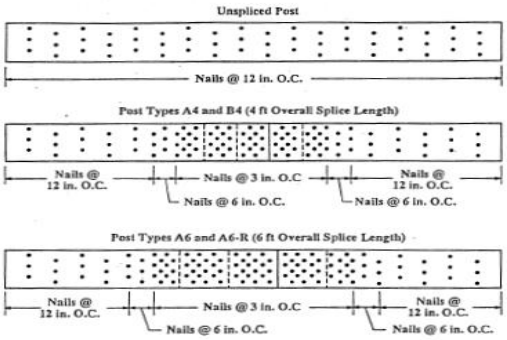

Figure 1 Pattern of strengthening without or with connections.

Table 1. Minimum space spikes (SNI 7973;2013)

	Wood Side Structure Components	
	Not drilled first	Drilled first
Edge Spacing	2.5D	2.5D
End Distance		
Fiber parallel pull load	15D	10D
Fiber parallel press load	10D	5D
Distance between fasteners in one row		
Fiber parallel	15D	10D
Perpendicular fiber	10D	5D
Distance between fastener rows		
Fiber parallel	5D	3D
Zig-zag	2.5D	2.5D

2. METHODS

The size of the wooden beam uses a model scale of 1:2 to overcome a wooden span that is too long so that the test object has a width (b) = 4 cm, beam height (h) = 6 cm with a span of 150 cm. For the arrangement of the lamina on the press and pull using meranti wood while the middle uses zircon wood. The height of each lamina is 2 cm. For adhesives between lamina, use nails with a diameter of 0.3 cm and used as a control variable.

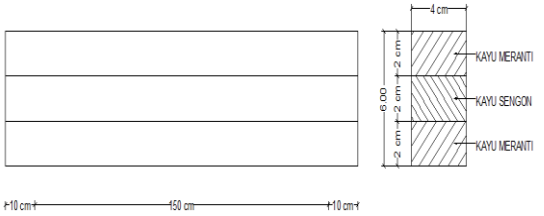

Figure 2 Lamina arrangement design of laminated wood beams.

The method of testing the characteristics of wood and the shape of the test object refers to the following standards:

1. Testing of Weight Characteristics, Moisture Content and Wood Levels (SNI 03-6844-2002 and PKK NI-5 1961)
2. Robust Characteristics Testing of Wood Press (SNI 03-3958-1995)
3. Vigorous Characteristics Testing of Wood Shear (SNI 03-3400-1994)
4. Complete Characteristics Testing of Bending Wood Beams (SNI 03-3959-1995)

Laminate beam test objects are made by varying the distance of the nail adhesive and ran to the supposition that the same risk profile can be applied to SFF. Therefore, factors like the Tip-Apex-Distance,

the Cleveland Directory, and reduction quality are considered risk factors for delayed fracture union in SFF [23]. Baumgaertner et al. described the measurement of TAD (tip-to-apex distance) to evaluate the placement of an SHS within the femoral head [24]. A major limiting factor is the cooling of adjacent plates as the distance from the spreading center or the plume increases, inhibiting their flexural capacities [25]. Information on the following variables was collected: number of blocking screws, the distance of each locking screw to osteotomy, distance of osteotomy from the joint line, and amount of lengthening [26]. and led to the assumption that the same risk profile can be applied to SFF. At the same time, we used a particular radiographic method optional by Lunsjo et al. and Serrano et al. to compute the distances of lag bolt sliding [27].

One test object treatment consists of three test objects with a dimension of width (b) = 4 cm, height (h) = 6 cm with varying nail distances, for the distance between joint-roller pedestals (L) = 150 cm. Each variation of the distance of the test object nails can be seen in Figure 3.

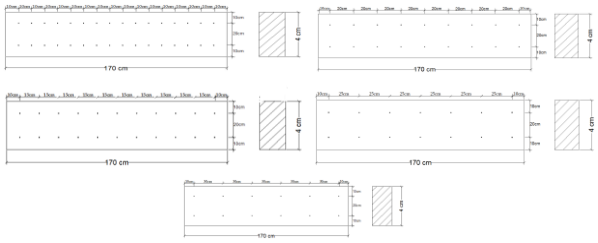

Figure 3 Design of distance variation of test object nails.

The one-point landing method performs the main test object testing of laminate beams. The placement of the dial gauge is designed with a clamp and magnet attached to the frame to stay in position and not shift when given loading. The dialing device placed the test object, two dial gauges are located in two long trees of right and left range, and one dial gauge is placed in a position right in the center of the content to read the magnitude of the deflection occurring at the time of charging.

Laminate beam test objects are drawn grids along the span before robust bending testing is carried out to make it easier to analyze the collapse pattern. The strong bending of the reflected rays in the gravitational field returns a significant fraction of the direct reflection to the disc to reflect the returning radiation. When illuminated by the primarily reflected emission, the plasma in the accretion disc produces a different spectrum when inspired by the power-law continuum spectrum. At the same time, time delays between higher-order reflections delay the average arrival time of the reverberating emission [28].

Below is an image of the setup testing bending wooden joint beams and the caption.

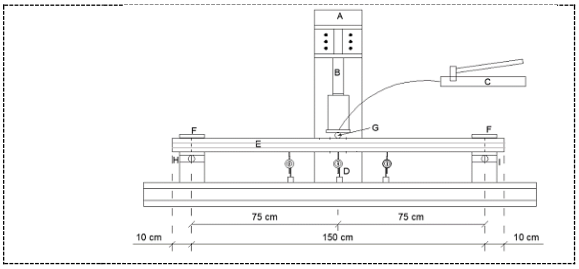

Figure 4 Set up bending beam testing objects.

Information:

A: *Loading Frame*
B: *Load Cell*
C: *Hydraulic Jack*
D: *Dial Gauge*
E: Wooden beams
F: Block clamp
G: Load distributor
H: Joint focus
I: Roller focus

3. RESULTS AND DISCUSSIONS

3.1 Characteristics of Wood Materials

Testing of wood characteristics aims to find out the wood material based on the physical properties of the wood and the mechanical properties of the wood. Wood that is done characteristic tester is the wood used to make the primary test material of mechanical-lamination beams and obtained from the same source. For the results of the test of the characteristics of meranti wood obtained the following results:

Table 2. Recapitulation of wood physical property testing results

No.	Test Object	Type Weight (gr/cm³)	Lehengas rate (%)	Water Content (%)
Sengon Wood		0.26	13.28	15.27
Meranti Wood		0.51	0.51	15.64

Table 3. Recapitulation of wood mechanical properties testing results

No.	Test Object	Strong Press (kg/cm²)	Strong Slide (kg/cm²)	Strong Bending (kg/cm²)
Sengon Wood		155,06	39,68	333.94
Meranti Wood		380,22	74,24	628.38

Based on the table above, according to PKKI NI-5-1961, strong press zircon wood falls into the category of solid grade IV wood, while meranti wood is included in the type of concrete class II wood.

3.2 The Capacity of Bending Beams

Testing is carried out on five laminate-mechanical wood beam test objects with different nail spacing. The data taken is a load with the condition of first crack (Pcrack) and maximum load beam (Pmax) to find out the effect of each variable on the loading that occurs. Here is a diagram of the loading of beams against variations in the distance of the nail.

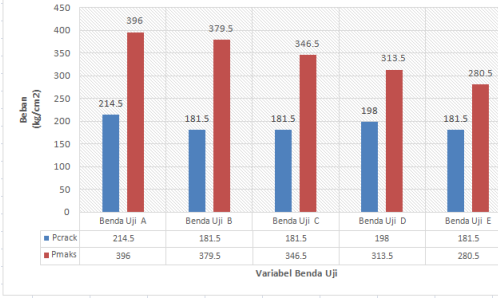

Figure 5 Comparison diagram of variables of test objects against loading.

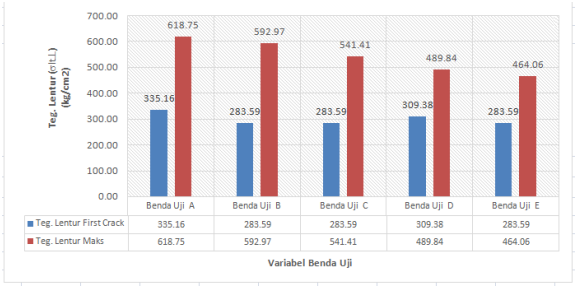

Figure 6 Strong comparison diagram of bending *first crack* conditions and maximum load (Pmax).

The diagram of the loading of the main test object beam against the bending loading obtained an extensive load at the time of first crack (Pcrack) and maximum loading (Pmax). The loading graph indicates that Test Object A (Nail Distance 10cm), Test Object B (Nail Distance 15cm), and Test Object C (Nail Distance 20cm) loading experienced a considerable increase. In comparison, the loading was relatively slightly increased for Test Object D (Nail Distance 25cm) and Test Object E (Nail Distance 30cm).

From the loading results, the loading will affect the strong bending of the beam. Based on the bending voltage equation described above, the decisive influence of bending the beam can be seen in Figure 6.

Bending voltage is obtained at maximum load conditions (Pmax) and first crack conditions. The diagram above shows that Test Object A (Nail Distance 10cm) has the highest bending voltage value among other test objects and is close to the strength of the base material of the outermost plywood, meranti wood. The lower but close test objects are Test Object B (15cm Nail Distance) and Test Object C (20cm). For Test Object D (Nail Distance 25cm) and Test Object E (Nail Distance 30cm), the value of bending voltage decreased considerably compared to other test objects.

A review was taken from the exposure to the load graph based on the same deflection, namely the permit deflection of 1/300 L (PKKI NI-5 1961 ps. 12.5), to show the beam strength of each variation.

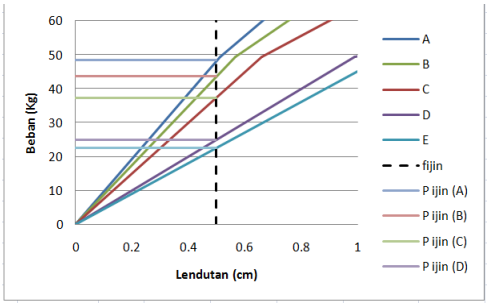

Figure 7 Graphic Details of Load and deflection Relationship Based on f = 0.5 cm.

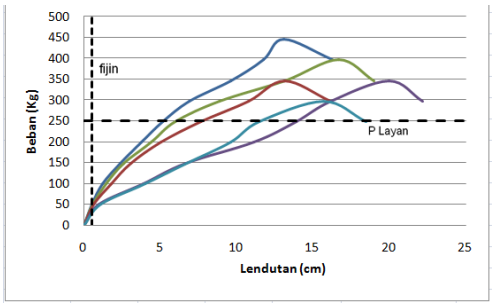

Figure 8 Graph of load relationships and deflection between variations.

The review was conducted based on a permit of 0.5cm, then Test Object A (Nail Distance 10cm) showed the highest loading. Test Object B (Nail Distance 15cm) and Test Object C (Nail Distance 20cm) has a lower loading value, but the difference is not too significant compared to Test Object A (Nail Distance 10cm). As for Test Object D (Nail Distance 25cm) and Test Object E (Nail Distance 30 cm), the load difference is quite far from other test objects.

Anticipate that the wood material of each beam has a different strength even though the same source is obtained; The power of the wood material used also affects bending.

3.3 Deflection Beam

The difference between the first crack and after the first crack is a deflection, but before the first crack and after the first crack still has a constant deflection because the beam is still elastic. Here are the results of the graph of the distribution of each variation.

From the results of the test objects on each variable obtained from the test results, the beam is still in an elastic condition where the graph shows the state that rises diagonally upwards. In addition, when the block is no longer flexible, the load can no longer increase, but the deflection continues to grow until the beam suffers a complete collapse.

Load exposure chart, review taken based on the same bag of 250 kg from the review, showing the best to the lowest level of rigidity of the test object.

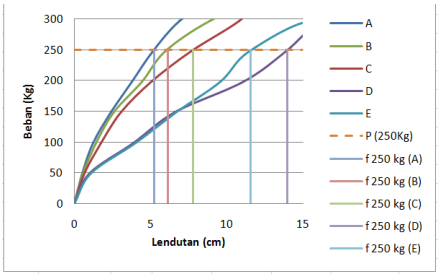

Figure 9 Graphic details of load and deflection relationships based on load (P = 250 kg).

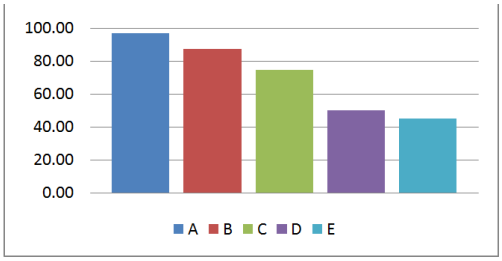

Figure 10 The grams stiffness values between variations.

Based on Figure 7 by comparing the same load (P= 250 kg), the lowest deflection is a test object with a distance between nails of 10cm. The long track length is used from the graph then the deflection gets bigger.

From the large deflection, the rigidity of a beam can be determined. The beam's rigidity is better if the shaft is experiencing a low deflection. Diagram of the rigidity value of variation, the longer the distance of the nail used, the smaller vale infallibility.

3.4 Laminate-Mechanical Beam Damage Analysis

Damage to each test object has different characteristics. Type of damage occurs with two kinds, namely bending and shear. Turning damage can be seen from the pattern of wood cracks that occur perpendicular to the fiber's direction or cut off the wood fiber. The sheer damage can be seen with the design of wood cracks that occur, leading horizontally or parallel to the direction of the thread where the wood fiber is in a detached condition.

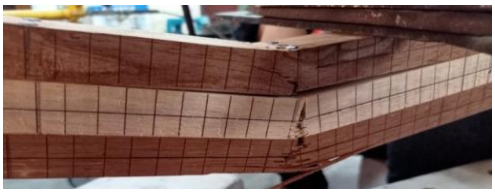

Figure 11 Type-A test object damage pattern (nail distance 10 cm).

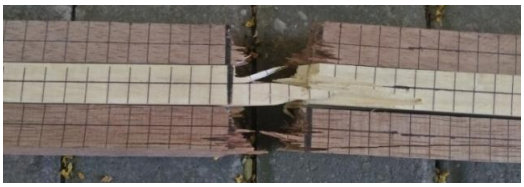

Figure 12 Type B test object damage pattern (nail distance 15 cm).

Test Object A (Nail Distance 10cm) damage occurs is bending damage where it can be seen that there is a crack that breaks the fiber in the area of attraction to the press area. Test Object B (Nail Distance 15cm) damage that occurs is also bending damage where it can be seen that there is a crack that cuts the fiber in the pull area to the press area. In this type of beam occurs loose between the lamination so that the strength of the beam cannot occur ultimately but detached between the lamination.

From the crack pattern of each test object, it can be seen that the more distance the nail used, the more damage is shear. It happens because the load of one claw to hold the horizontal derailment is getting bigger, which causes the beam not to work intact. Regardless of each lamination, the shaft can receive the bag is also getting smaller.

4. CONCLUSION

The distance of the nail as an adhesive on the laminate-mechanical wood beam affects the bending

strength. The greater the length of the pin used, the smaller the bending. It happens because glues, namely nails, cannot hold the horizontal Ferris between lamina, so it has not exceeded the maximum bending capacity obtained by the strength of the outer layer material of laminate-mechanical wood beams. The most optimal distance used on laminate-mechanical shafts is the 10cm nail distance. At that distance, the beam reaches 98% of the bending power against the bending strength of the primary material, namely meranti wood. It happens because the laminate-mechanical rays are still fused so that the beam is fully functional. Damage done to the test object shows that the greater the distance of the nail, the more damage that occurs leads to shear damage on mechanical laminate beams with nail spacing of 10cm and 15cm. It happens because the shaft is still fused at that distance so that the beam is still working fully.

AUTHORS' CONTRIBUTIONS

Suprapto: data analysis, experimenting. Supari: review manuscript and supervisor. Ekohariadi: review manuscript and supervisor. Reza Bagus Aditya: review manuscript and supervisor; and Setya Chandra Wibawa: review manuscript and supervisor.

REFERENCES

[1] T. Zhou *et al.*, "Super-tough MXene-functionalized graphene sheets," *Nat. Commun.*, vol. 11, no. 1, pp. 1–11, 2020, doi: 10.1038/s41467-020-15991-6.

[2] O. Platnieks *et al.*, "Highly loaded cellulose/poly (butylene succinate) sustainable composites for woody-like advanced materials application," *Molecules*, vol. 25, no. 1, 2020, doi: 10.3390/molecules25010121.

[3] S. Razavi Bazaz *et al.*, "3D Printing of Inertial Microfluidic Devices," *Sci. Rep.*, vol. 10, no. 1, pp. 1–14, 2020, doi: 10.1038/s41598-020-62569-9.

[4] S. Wear, C. Al, and C. Al O, "Comparative Study on the Cavitation Erosion and," 2020.

[4] M. Szala., L. Łatka., M. Walczak., and M. Winnicki,. Comparative Study on the Cavitation Erosion and Sliding Wear of Cold-Sprayed Al/Al_2O_3 and Cu/Al_2O_3 Coatings, and Stainless Steel, Aluminium Alloy, Copper and Brass. *Metals 10*, 856., 2020, DOI: https://doi.org/10.3390/met10070856

[5] A. Capatina, V. Bria, M. Bunea, and I. G. Birsan, "Tensile behaviour of fabric reinforced laminates and plies," *Mater. Plast.*, vol. 56, no. 2, pp. 370–377, 2019, doi: 10.37358/mp.19.2.5188.

[6] A. Siddika *et al.*, "Performance of sustainable green concrete incorporated with fly ash, rice husk ash, and stone dust," *Acta Polytech.*, vol. 61, no. 1, pp. 279–291, 2021, doi: 10.14311/AP.2021.61.0279.

[7] Q. Cheng *et al.*, "Achromatic terahertz Airy beam generation with dielectric metasurfaces," *Nanophotonics*, vol. 10, no. 3, pp. 1123–1131, 2021, doi: 10.1515/nanoph-2020-0536.

[8] M. C. Arno *et al.*, "Exploiting the role of nanoparticle shape in enhancing hydrogel adhesive and mechanical properties," *Nat. Commun.*, vol. 11, no. 1, 2020, doi: 10.1038/s41467-020-15206-y.

[9] D. Gan *et al.*, "Mussel-Inspired Redox-Active and Hydrophilic Conductive Polymer Nanoparticles for Adhesive Hydrogel Bioelectronics," *Nano-Micro Lett.*, vol. 12, no. 1, pp. 1–16, 2020, doi: 10.1007/s40820-020-00507-0.

[10] J. Alberto *et al.*, "Fully Untethered Battery-free Biomonitoring Electronic Tattoo with Wireless Energy Harvesting," *Sci. Rep.*, vol. 10, no. 1, pp. 1–11, 2020, doi: 10.1038/s41598-020-62097-6.

[11] X. Meng *et al.*, "Bio-inspired vertebral design for scalable and flexible perovskite solar cells," *Nat. Commun.*, vol. 11, no. 1, pp. 1–10, 2020, doi: 10.1038/s41467-020-16831-3.

[12] X. Chen, H. Yuk, J. Wu, C. S. Nabzdyk, and X. Zhao, "Instant tough bioadhesive with triggerable benign detachment," *Proc. Natl. Acad. Sci. U. S. A.*, vol. 117, no. 27, pp. 15497–15503, 2020, doi: 10.1073/pnas.2006389117.

[13] P. M. S. Shimabukuro *et al.*, "Environmental cleaning to prevent COVID-19 infection. A rapid systematic review," *Sao Paulo Med. J.*, vol. 138, no. 6, pp. 505–514, 2020, doi: 10.1590/1516-3180.2020.0417.09092020.

[14] K. Polhun, T. Kramarenko, M. Maloivan, and A. Tomilina, "Shift from blended learning to distance one during the lockdown period using Moodle: Test control of students' academic achievement and analysis of its results," *J. Phys. Conf. Ser.*, vol. 1840, no. 1, 2021, doi: 10.1088/1742-6596/1840/1/012053.

[15] C. Xu and L. Zhang, "Application of XR-Based Virtuality-Reality Coexisting Course," *Intell. Autom. Soft Comput.*, vol. 31, no. 3, pp. 1843–1855, 2022, doi: 10.32604/iasc.2022.020365.

[16] E. M. Tudor, M. C. Barbu, A. Petutschnigg, R. Réh, and Ľ. Krišťák, "Analysis of larch-bark capacity for formaldehyde removal in wood adhesives," *Int. J. Environ. Res. Public Health*, vol. 17, no. 3, 2020, doi: 10.3390/ijerph17030764.

[17] M. A. Oyarhossein *et al.*, "Dynamic response of the nonlocal strain-stress gradient in laminated polymer composites microtubes," *Sci. Rep.*, vol. 10, no. 1, pp. 1–19, 2020, doi: 10.1038/s41598-020-61855-w.

[18] P. Li *et al.*, "Continuous crystalline graphene papers with gigapascal strength by intercalation modulated plasticization," *Nat. Commun.*, vol. 11, no. 1, pp. 1–10, 2020, doi: 10.1038/s41467-020-16494-0.

[19] A. S. Mostovoy, M. A. Vikulova, and M. I. Lopukhova, "Reinforcing effects of aminosilane-functionalized h-BN on the physicochemical and mechanical behaviors of epoxy nanocomposites," *Sci. Rep.*, vol. 10, no. 1, pp. 1–11, 2020, doi: 10.1038/s41598-020-67759-z.

[20] O. J. Shon, C. H. Choi, and C. H. Park, "Factors associated with mechanical complications in intertrochanteric fracture treated with proximal femoral nail antirotation," *Hip Pelvis*, vol. 33, no. 3, pp. 154–161, 2021, doi: 10.5371/HP.2021.33.3.154.

[21] H. Yang *et al.*, "Carbon dioxide electroreduction on single-atom nickel decorated carbon membranes with industry compatible current densities," *Nat. Commun.*, vol. 11, no. 1, pp. 1–8, 2020, doi: 10.1038/s41467-020-14402-0.

[22] S. Wan *et al.*, "Strong sequentially bridged MXene sheets," *Proc. Natl. Acad. Sci. U. S. A.*, vol. 117, no. 44, pp. 27154–27161, 2020, doi: 10.1073/pnas.2009432117.

[23] V. Freigang *et al.*, "Risk factor analysis for delayed union after subtrochanteric femur fracture: Quality of reduction and valgization are the key to success," *BMC Musculoskelet. Disord.*, vol. 20, no. 1, pp. 1–8, 2019, doi: 10.1186/s12891-019-2775-x.

[24] G. Gargano, N. Poeta, F. Oliva, F. Migliorini, and N. Maffulli, "Zimmer Natural Nail and ELOS nails in pertrochanteric fractures," *J. Orthop. Surg. Res.*, vol. 16, no. 1, pp. 1–9, 2021, doi: 10.1186/s13018-021-02634-9.

[25] D. Arcay, S. Lallemand, S. Abecassis, and F. Garel, "Can subduction initiation at a transform fault be spontaneous?," *Solid Earth*, vol. 11, no. 1, pp. 37–62, 2020, doi: 10.5194/se-11-37-2020.

[26] S. Dabash, D. T. Zhang, S. R. Rozbruch, and A. T. Fragomen, "Blocking screw-assisted intramedullary nailing using the reverse-rule-of-thumbs for limb lengthening and deformity correction," *Strateg. Trauma Limb Reconstr.*, vol. 14, no. 2, pp. 77–84, 2019, doi: 10.5005/jp-journals-10080-1430.

[27] S. Oh, Y. S. Kim, S. Y. Kwon, J. Jung, C. Yoon, and J. H. Song, "Additional use of anti-rotation U-blade (RC) decreases lag screw sliding and limb length inequality in the treatment of intertrochanteric fractures," *Sci. Rep.*, vol. 11, no. 1, pp. 1–10, 2021, doi: 10.1038/s41598-021-96988-z.

[28] D. R. Wilkins, J. A. Garciá, T. Dauser, and A. C. Fabian, "Returning radiation in strong gravity around black holes: Reverberation from the accretion disc," *Mon. Not. R. Astron. Soc.*, vol. 498, no. 3, pp. 3302–3319, 2020, doi: 10.1093/mnras/staa2566.